Molten chloride salts for high-temperature thermal energy storage: Continuous electrolytic salt purification with two Mg-electrodes and alternating voltage for corrosion control

Wenjin Ding[a,*], Fan Yang[a], Alexander Bonk[a], Thomas Bauer[b]

[a]*Institute of Engineering Thermodynamics, German Aerospace Center (DLR), Stuttgart, Germany*

[b]*Institute of Engineering Thermodynamics, German Aerospace Center (DLR), Cologne, Germany*

*Corresponding author. Tel.: +49 711 686 2233. E-mail address: wenjin.ding@dlr.de.

Abstract

Molten chloride salts such as $MgCl_2$/KCl/NaCl are promising thermal energy storage (TES) materials and heat transfer fluids (HTF) in next generation concentrated solar power (CSP) plants with elevated operation temperatures (> 700°C) due to their high thermal stability and low material costs. However, they have strong corrosivity against metallic structural materials at high temperatures which can be related to the presence of hydrolysis products such as MgOHCl. In an electrolytic purification method reported in previous work, a W-cathode and Mg-anode were used to reduce the concentration of these impurities, thereby effectively purifying the molten $MgCl_2$/KCl/NaCl salt. However, the W-cathode passivation due to production of MgO on the surface limited its cathode effectiveness. In this work, an improved electrolytic purification method is presented to avoid the electrode passivation by using two identical Mg-electrodes and alternating voltage (AV, i.e., switching the voltage direction applied periodically). A continuous electrolytic salt purification in the AV-mode is successfully performed on the molten $MgCl_2$/KCl/NaCl salt in the 100 g-scale. Cyclic voltammetry (CV) on the molten salt shows that the purification can effectively reduce the concentration of the main corrosive impurity $MgOH^+Cl^-$. Potentiodynamic polarization (PDP) measurements on a commercial alloy (Incoloy 800 H) immersed in the molten salt indicate significantly reduced corrosion rates (i.e., reduced salt corrosivity) compared to a non-purified salt. The continuity of the improved method allows for a long-term effective purification without the risk of passivation and deactivation of electrodes, thereby showing great potential in corrosion control of molten chloride salt TES system.

Keywords

Concentrated solar power (CSP); Continuous salt purification; Corrosive impurity; Electrolysis; Electrode passivation; Thermal energy storage (TES).

1. Introduction

Next generation concentrated solar power (CSP) plants with higher thermal-to–electrical energy conversion envisage operation temperatures of > 700 °C thereby creating a demand for thermal energy storage (TES) media and heat transfer fluids (HTF) with higher operation temperatures than currently utilized nitrate salt mixtures [1-8]. Molten chloride salt mixtures (e.g., $MgCl_2$/KCl/NaCl, $CaCl_2$/KCl/NaCl, $ZnCl_2$/KCl/NaCl, $MgCl_2$/NaCl) are promising TES and HTF materials in the next generation CSP plants, due to their excellent thermal properties (e.g., high thermal stability of >800 °C), high abundancy and low material costs [1-8]. In order to promote the development of the next generation CSP plants, the US Department of Energy (DOE) has started the Generation 3 Concentrating Solar Power Systems (Gen3 CSP) program in May of 2018 [10], in which molten chloride salts are being extensively studied as one of the most promising TES and HTF materials [1,11,12]. Besides US, some research institutions in other countries and regions (e.g., Australia, China, Europa) investigate molten chloride salts for next generation CSP plants [2,13-16].

However, the application of molten chloride salts at high temperatures is limited by some factors, particularly their high melting points as well as their strong corrosivity against structural materials, compared to the commercial TES/HTF molten nitrate salts [1, 8]. In order to reduce the melting temperatures of the chloride salt mixtures and keep low material costs, some alkaline earth metal chloride salts (e.g., $MgCl_2$ and $CaCl_2$) or $ZnCl_2$ are added into the alkali metal chloride salts or salt mixtures (e.g., NaCl, KCl, NaCl/KCl) [17]. Among them, the low-cost (<0.35 USD/kg) low-melting-temperature (~385°C) $MgCl_2$/KCl/NaCl salt mixture is extensively investigated as one of the most promising candidates of next generation TES/HTF materials [2,4,8,12-13,16-17]. However, $MgCl_2$ salt is strongly hygroscopic and can be hydrated after a short contact with ambient air. The hydrated compounds in turn are hydrolyzed during heating/melting to form corrosive HCl and hydroxide species such as MgOHCl, which are dissolved in the melt in form of $MgOH^+Cl^-$ [14, 16-18]. Current research aims at developing reliable, effective and affordable corrosion control methods [15-24]. It is accepted that the corrosion of structural materials (e.g., commercial Fe-Cr-Ni alloys) in molten chlorides is mainly driven by aforementioned hydroxyl-based impurities (e.g. hydroxychlorides, $MgOH^+Cl^-$) but also oxygen gas dissolved in the molten chloride salts [16-18]. These corrosive impurities in the molten salt react with (i.e., corrode) the containers and structural materials, if they are not removed. More about the corrosion behaviors and mechanisms of Cr-Fe-Ni alloys in molten chloride salts can be found in open literature [8,16-24, 25-26].

In order to realize the commercial application of molten chloride salts at high temperatures, some techniques for reducing their corrosivity [24,25,27-36] or increasing corrosion resistance of the structural materials [37-40] have been investigated. These techniques, summarized in Table 1, involve: 1) salt purification to reduce the corrosive impurities, 2) modification of the alloys to produce a protective layer on the surface. The corrosive impurities in the molten chloride salts can be reduced by chemical, electrochemical or thermal means. Alloy protection can be achieved by different techniques, but most of them ultimately result in the formation of a corrosion-resistant (outward-facing) Al_2O_3 layer which is in contact with the molten chloride salts. Such alumina layer can be produced by coating an Al-containing layer on the alloys and oxidizing it to Al_2O_3, or by pre-oxidizing Al-containing alloys (e.g. FeCrAl).

Table 1: Available techniques for reducing corrosion rates of structural metals in molten chlorides.

Technique on	**Type**	**Example**
Salt purification	Chemical	• bubbling with chlorinating compounds such as CCl_4, HCl [25,27-29]
		• Adding active metals such as Mg and Li [30-34]
	Electrochemical	• Electrolysis with various electrodes such as W, Mg [24, 41]
	Thermal	• Stepwise heating [35-36]
Alloy modification	Al-containing coatings	• Oxidation of Al-containing coatings [37-38]
	Al-containing alloys	• Pre-oxidation of Al-containing alloys [39-40]

As a common electrochemical method, the electrolysis with two inert electrodes (e.g., tungsten W [41-44]) or one inert cathode + one 'active' anode (e.g., inert cathode + graphite anode [45]) has been investigated and used for purification of molten chloride salts. Here, the 'activity' of the electrode means the electrode material can react with the species in the melt during the electrolysis. In our previous work an electrolytic salt purification method (using direct voltage, DV) was investigated for the molten $MgCl_2$/KCl/NaCl salt [24]. An active Mg-anode and an inert W-cathode were used in this method to reduce corrosive impurities in the molten salt, mainly the aforementioned $MgOH^+Cl^-$. For evaluating the salt purification effectiveness, cyclic voltammetry (CV) developed in previous work [41-42] was used to measure the impurity concentration of the molten chloride salt, while the potentiodynamic polarization (PDP) method [24] was used to estimate the corrosion rates of a commercial high-temperature alloy (Incoloy 800 H) immersed in the purified and unpurified molten chloride salt. The results showed that this method could effectively reduce the concentration of the impurity $MgOH^+Cl^-$, thus the corrosivity of the molten salt. However, steady passivation of the W-cathode due to the

production of MgO on its surface limited the continuity of the purification method, since the MgO passivation layer on the cathode had to be removed regularly.

In the present paper, an improved electrolytic salt purification method for the molten chlorides is investigated using two identical Mg-electrodes and alternating voltage (AV). This method is expected to improve the purification duration by slowing down the electrode passivation. A continuous electrolytic salt purification of 2 hours based on this method is performed. As in previous work [24], CV on the molten salt and PDP measurements on an Incoloy 800 H (In 800 H) alloy sample immersed in the molten salt are performed to validate the purification effect. Moreover, the mechanism of the improved electrolytic purification is investigated.

2. Experimental

2.1. Experimental set-up

Figure 1 shows a schematic of the experimental set-up used for the salt electrochemical purification using two identical Mg-electrodes (purity ≥ 99.5%, *Sigma Aldrich*, Germany) as well as for CV and PDP experiments, described in more detail elsewhere [24]. The CV method has been used in previous work [24] to study the effect of salt purification on reduction of salt corrosivity. It was developed in our previous work [41-42] for monitoring the concentration of the main corrosive impurity $MgOH^+$ in an in-situ corrosion control system, and has been calibrated with a post-analysis method based on titration. It was shown that the height of the current peak representing the reduction reaction of $MgOH^+$ in CV was proportional to the bulk concentration of $MgOH^+$ in the molten salt. Thus, in this work, instead of the chemical post-analysis on salt samples, CV was used for in-situ test the purity of the molten salt before and after salt purification, in order to avoid the entrance of air into the autoclave during the salt sampling. More details about CV (calculation of impurity concentration) and PDP experiments (calculation of corrosion rate) can be found in our previous work [24]. The salt electrochemical purification used in this work will be introduced in Section 3.1 in detail. A glassy carbon crucible (*HTW* Germany, Sigradur® G) was used to avoid the reaction of the molten chloride salt with the crucible material. During the experiments, the temperature of the molten salt in an argon atmosphere (5.0 grade) was controlled by the programmable furnace and the thermocouple located close to the molten salt surface (see Figure 1). For electrochemical experiments, an Al_2O_3 plate was used under the glassy carbon crucible to electrically isolate it from other metallic parts of the experimental set-up.

As shown in Figure 1, six electrodes were used for the electrochemical purification, CV and PDP experiments. Table 2 shows which electrodes were used in each experiment and which

materials were used for the electrodes. A tungsten electrode immersed in the molten salt was used as the quasi-reference electrode for the CV and PDP experiments. In this work, two identical Mg-electrodes (Electrode e and f) were polished with sandpapers (600, 800 and 1200#) to remove the MgO layer on the surface and connected with the tungsten wire (see Figure 2 left). The Incoloy 800 H (In 800 H: Ni29.40-Cr20.84-Mn1.06-Si0.78) electrodes (see Figure 2 right) were polished with sandpapers (600, 800 and 1200#), and washed by distilled water and acetone, in order to have mirror-like clean surfaces.

All the electrochemical experiments were conducted using a ZENNIUM electrochemical workstation from *Zahner GmbH* (Germany). All the pure tungsten wires used in this work, as the electrodes or electrode parts, were purchased from *Alfa Aesar* (purity ≥ 99.95 %, diameter: 1 mm). In the CV experiments, the immersion depth of the working tungsten electrode was fixed to 5 mm by using an ohmmeter (i.e., the contact area of the tungsten electrode with the melt is ~16.5 mm^2), while the counter and reference electrodes had a much larger immersed area, as shown in Figure 1. In the PDP experiments, the contact area of the In 800 H electrode with the melt is ~7 cm^2.

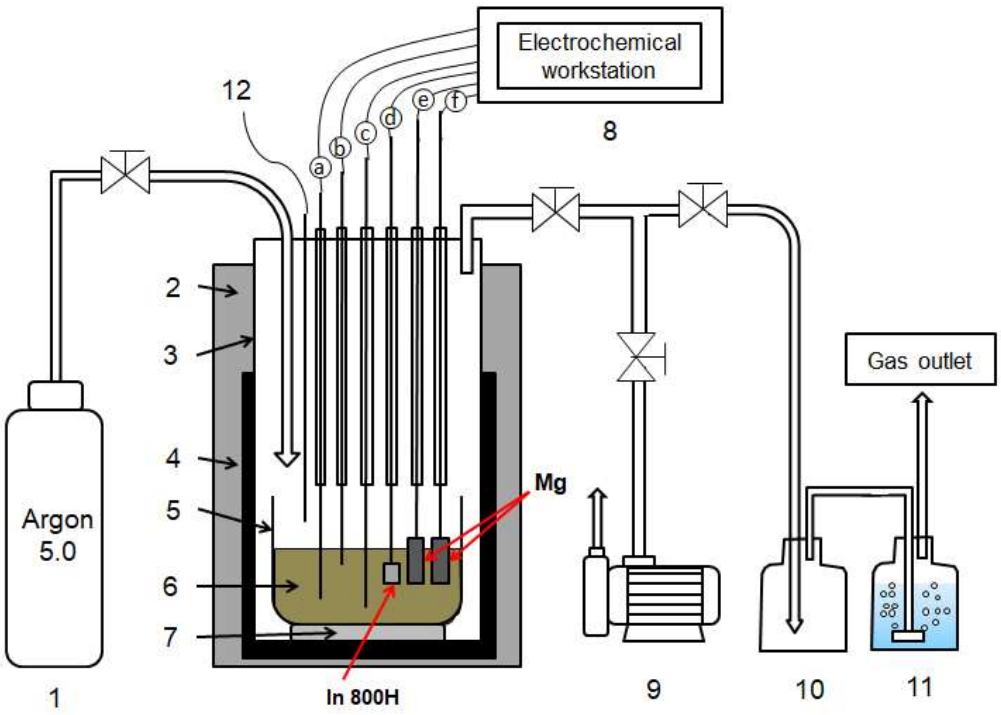

Figure 1: Schematic of experimental set-up for electrochemical salt purification with two identical Mg-electrodes, CV and PDP experiments. 1: Storage tank for argon 5.0 gas, 2: Glass wool heat isolator, 3: Steeling tube of In 800 H, 4: Furnace, 5: Glassy carbon crucible, 6: Molten chloride salt, 7: Al_2O_3 plate, 8: Electrochemical workstation for electrochemical experiments, 9: Vacuum pump, 10: Security bottle (empty) for reflux from the bottle for gas washing, 11: Bottle with NaOH solution for gas washing (removal of HCl and Cl_2), 12: Thermocouple close to the molten salt.

Table 2: Electrodes used for electrochemical purification, CV and PDP measurements.

Experiments	Applications	Electrode identified in Figure 1		
		Working	Counter	Reference
Electrolysis	Electrochemical purification with AV	f/e	e/f	e/f
CV	Measuring impurity concentration	b	c	a
PDP	Corrosion potential / rate of studied alloy	d	c	a

Electrodes:

a: Tungsten quasi-reference electrode,

b: Tungsten working electrode,

c: Tungsten counter electrode,

d: Alloy sample (In 800 H, 1×1×1.5 cm) + tungsten wire,

e: Mg-1 electrode, Mg-rod (diameter: 6.15 mm, length: 50 mm) + tungsten wire for salt purification,

f: Mg-2 electrode, same as Mg-1 electrode.

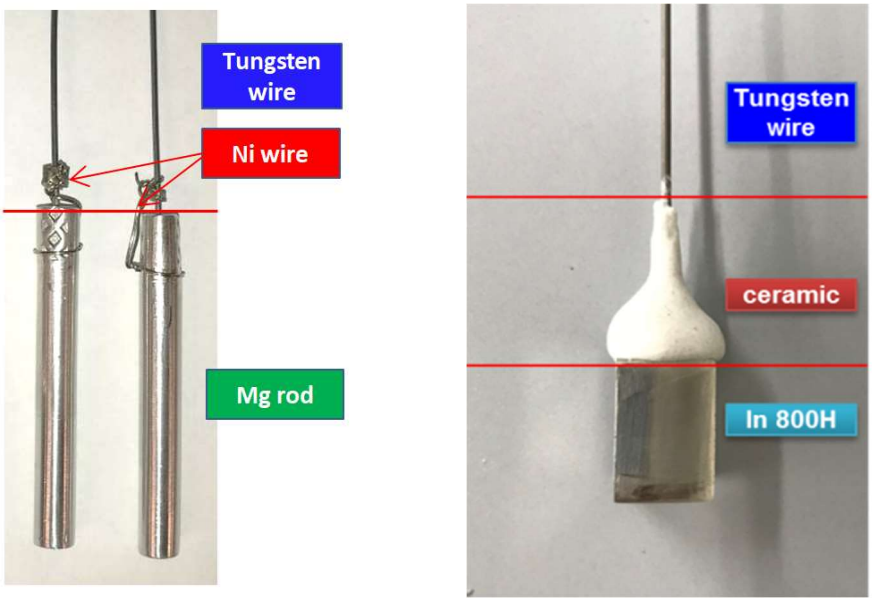

Figure 2: Left: Magnesium electrodes; Right: Electrode with In 800 H sample. For Mg electrodes, the Mg rods were bond with a tungsten wire via a hole in the Mg rods and cold compression, and with an additionally supporting Ni wire. The In 800 H sample was bond with a tungsten wire, and the bonding point was covered with silicon ceramic (*Aremco* 645-N) to avoid the molten salt entering the bonding point.

2.2. Experimental procedures

KCl (purity ≥ 99%, *Alfa Aesar*, Germany) and NaCl (purity ≥ 99%, *Alfa Aesar*, Germany) were purchased, while anhydrous $MgCl_2$ (purity ≥ 99%) was purchased from *Magnesia*, Germany. The anhydrous $MgCl_2$ has a small amount of hydrated water (~1%) due to its strong

hygroscopicity and short contact with air. They were used to synthesize the salt mixture of $MgCl_2$/KCl/NaCl (60/20/20 mol. %, melting temperature ~400°C). The heating process of the salts in this work was identical as that reported in our previous work [24]: after vacuuming by the vacuum pump for 30 minutes (≤ 30 mbar), the salt mixture (~140 g) was heated (heating rate of ~5°C/min) under an argon atmosphere (Argon 5.0, purity ≥ 99.999%, H_2O ≤ 3 ppm, O_2 ≤ 2 ppm, 30 NL/h, pressure above atmospheric pressure is about 0.1 bar) to 200°C, then held at 200°C for 1 hour to release the hydrated water and to reduce the side reaction to hydroxides (e.g., MgOHCl) and HCl. After that, the salt was heated to 500°C (heating rate of ~5°C/min) for salt purification. Before the salt purification, the concentration of the corrosive impurity $MgOH^+$ was measured with CV, while the corrosion rate of the In 800 H electrode as shown in Figure 2 right was measured with PDP. After the PDP measurement, the In 800 H electrode was moved out of the molten salt in order to avoid the reaction with the corrosive impurities during the salt purification. Then, the two identical Mg-electrodes as shown in Figure 2 left were immersed into the molten salt, and the salt purification experiment was performed for two hours. The concentration of the corrosive impurity and the corrosion rate of Incoloy 800 H were measured again with the CV and PDP method, respectively, in order to investigate the salt purification effect.

3. Results and discussion

3.1. Proposed mechanism and pre-experiments of electrolytic salt purification using two identical Mg-electrodes and alternating voltage (AV)

In the electrolytic salt purification method investigated in this work, AV is applied on the two identical Mg-electrodes to remove the main corrosive impurity $MgOH^+$ in the molten salt, as shown in Figure 3. These two magnesium electrodes are indicted with Mg-1 and Mg-2, respectively. The AV is defined in a square wave form (Phase 1: positive voltage; Phase 2: negative voltage) shown in Figure 4, in order to better investigate the effect of AV on reduction of electrode passivation.

In Phase 1 (Figure 3 left), Mg-1 serves as the cathode, while Mg-2 serves as the anode. As depicted in Figure 3 left, the following reactions occur at the cathode and anode during the electrolytic salt purification, respectively:

Cathode (Reduction):	$2MgOH^+ + 2e^- \rightarrow 2MgO(s) + H_2(g)$	(I)
Anode (Oxidation):	$Mg(s) - 2e^- \rightarrow Mg^{2+}$	(II)
Total Reaction:	$2MgOH^+ + Mg(s) \rightarrow Mg^{2+} + 2MgO(s) + H_2(g)$	(III)

In Reaction (I) on the cathode, as MgO is hardly soluble in the molten chloride salts [41], it either remains at the electrode or precipitates in the molten salt. Since MgO is none electrically conductive, remaining at the electrode leads to electrode passivation, and significantly reduces the current. At the Mg anode, Mg^{2+} is formed leading to a steady consumption of the anode. In Phase 2 as the voltage applied on the Mg-electrodes is switched (see Figure 4), the Mg cathode in Phase 1 (Mg-1) now serves as the anode, while Mg-2 serves as the cathode. Thus, the insoluble MgO formed primarily on the Mg-1 surface detaches due to the dissolution of the subjacent Mg-electrode according to reaction (II). By repetition of the voltage switch (i.e., repeating Phase 1 and 2), the electrode passivation can be effectively reduced, and the purification duration can be improved. The experimental observations and results supporting the proposed mechanism of this improved salt purification will be reported in Sections 3.2 and 3.3.

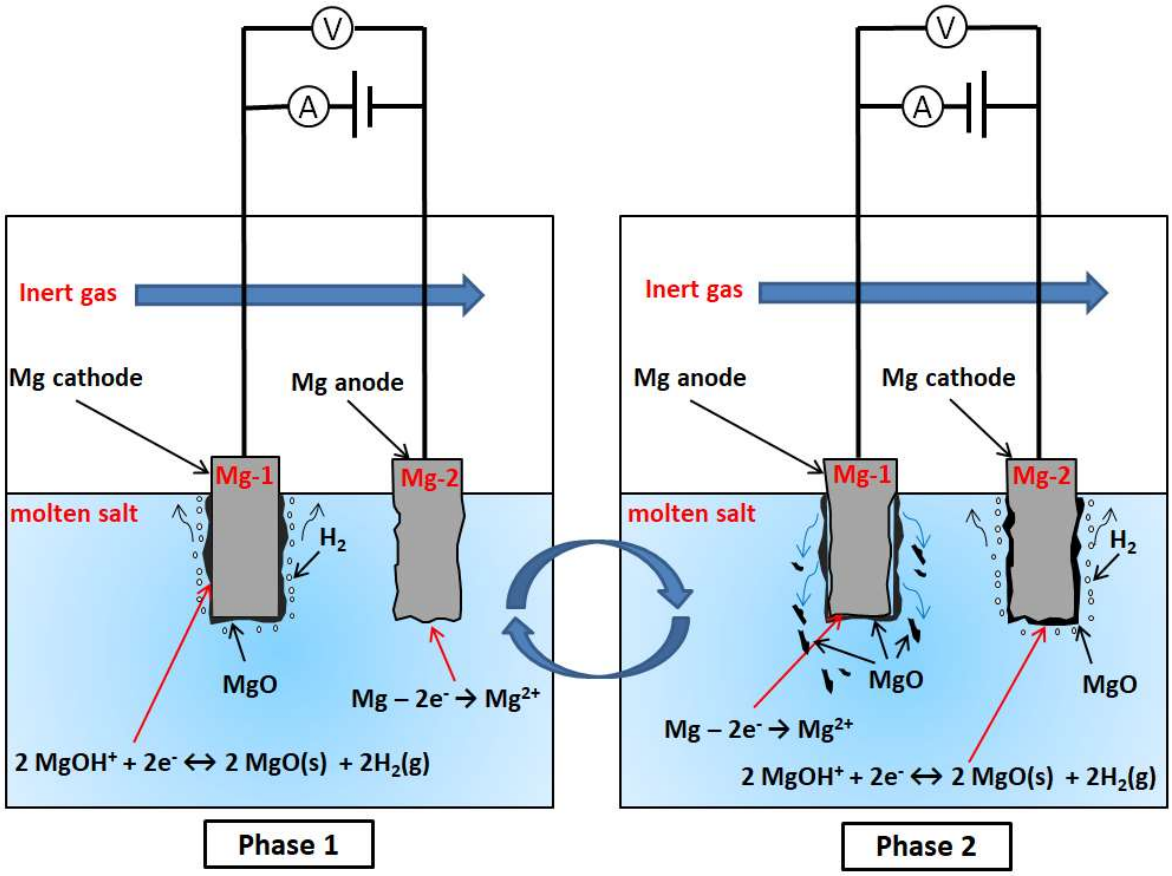

Figure 3: Electrochemical salt purification using two identical Mg electrodes as the cathode and anode with periodically switched polarization of the voltage (i.e., AV) to slow down the cathode passivation by the produced MgO. Left (Phase 1): Removal of impurity and production of MgO on the cathode; Right (Phase 2): Falling-off of MgO on the electrode due to Mg → Mg^{2+} dissolution.

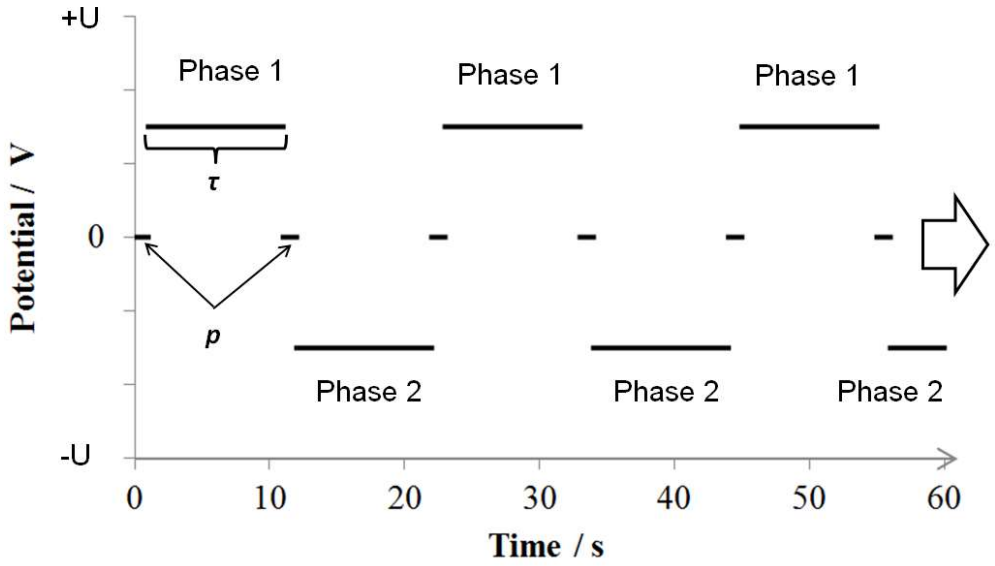

Figure 4: Alternating voltage (AV) applied on Mg electrodes in a square signal form with amplitude (*U*), time interval (τ) and short pause (*p*). Here, the time interval (τ) means the duration of one electrolysis phase. Between Phase 1 and 2, a pause (*p*) of 1 second was set for all tests to avoid current overload due to fast changes of the voltage.

Prior to the continuous electrolytic salt purification, various conditions with different amplitude (*U*) and time interval (τ) were investigated to find the suitable conditions. Since a too high voltage $U > 1.0$ V and a too long time interval $\tau > 10$s may lead to unexpected side-reactions and irreversible electrode passivation, six pre-experiments with different *U* (0.2-1.0 V) and τ (2-10 s) were conducted at 500°C. Based on the results of pre-experiments, the conditions of $U = 0.8$ V and $\tau = 2$ second were chosen for the continuous electrolytic salt purification experiment regarding high electrolysis current and low electrode passivation rate. Figure 5 shows the change of electrolysis current vs. time in the pre-experiment under the conditions of $U = 0.8$ V and $\tau = 2$ s. The pre-experiments (as presented in Figure 5) show a steady but slow decrease of the current with the electrolysis time due to the electrode passivation. Moreover, when the time interval τ is ≤ 2 s for $U = 0.8$ V, the current shows no decrease within one time interval owing to falling-off of MgO on the anode.

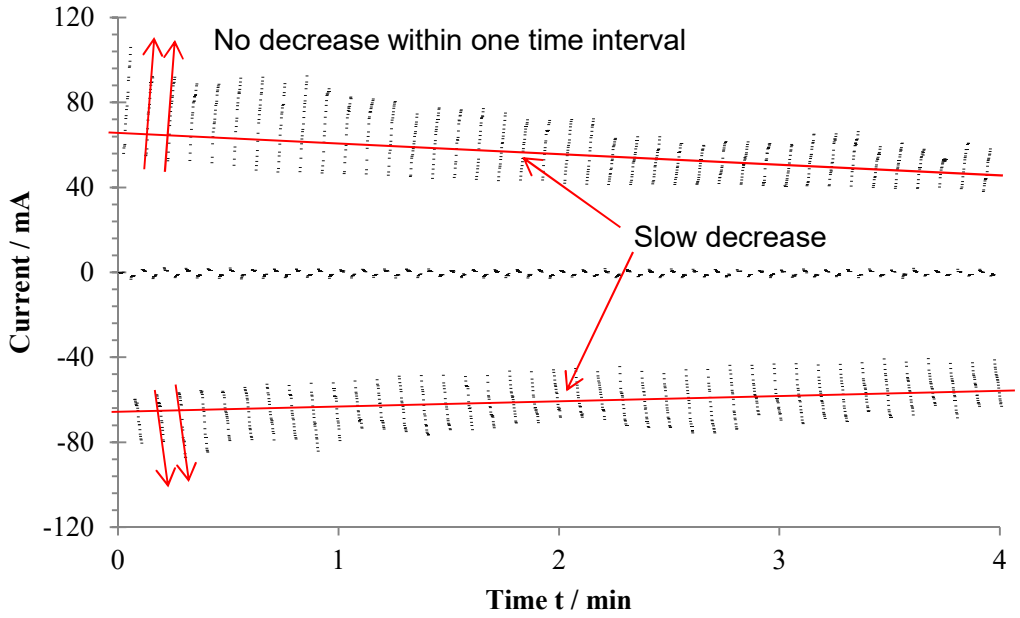

Figure 5: Current vs. time of the pre-experiment under the conditions of U = 0.8 V and τ = 2 s.

3.2. Electrolytic salt purification on molten chlorides for 2 hours

Under the chosen conditions (U = 0.8 V, τ = 2 s and p = 1 s), up to 2 hours electrolytic salt purification with two identical Mg electrodes was performed on the molten $MgCl_2$/KCl/NaCl salt (60/20/20 mol.%) at 500°C. As shown in Figure 6, a strong current drop was observed on the initial stage (t < 20 min). This can be explained by the fast decrease of the impurity concentration due to high rate of the salt purification (high current). After the initial stage, the current decrease would be slower due to the low impurity concentration and/or the partial electrode passivation caused by the electrolysis product MgO. During the experiment, some instantaneous increases of the current were observed in Figure 6. Our previous work [24] shows that the salt purification with a Mg-anode and a W-cathode using a non-switching potential (i.e., DV), the electrolysis stopped within 5 min due to the complete passivation of the W-cathode. The results in this work show significant improvement in electrolysis duration.

Figure 7 shows an image of the two magnesium electrodes and salt residues on the electrode surface after the 2 h salt purification test. The salt residues on the two electrodes were not strongly adherent and could be peeled off easily. This complements the findings described earlier that electrodes recover when switching from cathode- to anode-mode (Figure 3). It may be expected that the anode reaction from Mg to Mg^{2+} can easily occur under this residual MgO-layer. After removing the residual layers on the two electrodes, the parts of these electrodes immersed in the molten salt for the salt purification show a blank metal surface indicating the

presence of metallic magnesium rather than a white appearance with adherent MgO. This observation can explain the repetitive instantaneous increases of the current shown in Figure 6 during the 2 h experiment. The salts residual on the electrodes were analyzed with X-ray diffraction (XRD). The XRD analysis results in Figure 8 show that both salts residual on Mg-1 and Mg-2 contain a large amount of the electrolysis product MgO, confirming that passivation occurs during the cathodic reaction at the respective electrode.

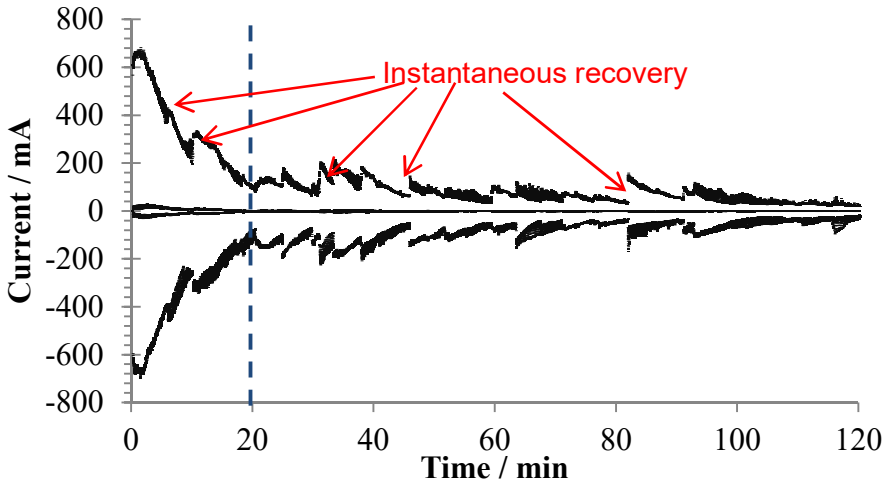

Figure 6: Current vs. time t in 2 hours salt purification under the conditions U = 0.8 V, τ = 2 s and p = 1 s.

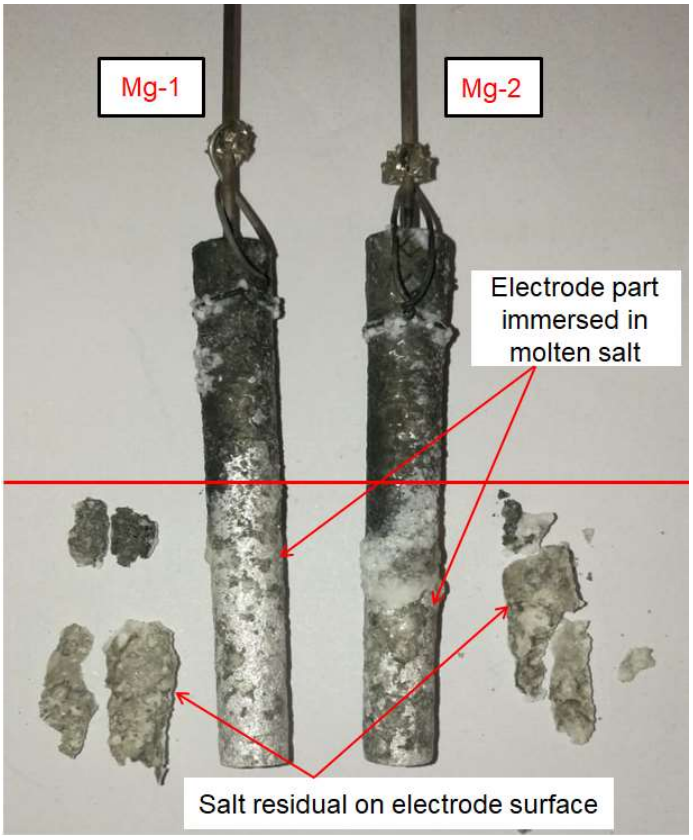

Figure 7: Image of magnesium electrodes and salt residual on electrode surface after salt purification test.

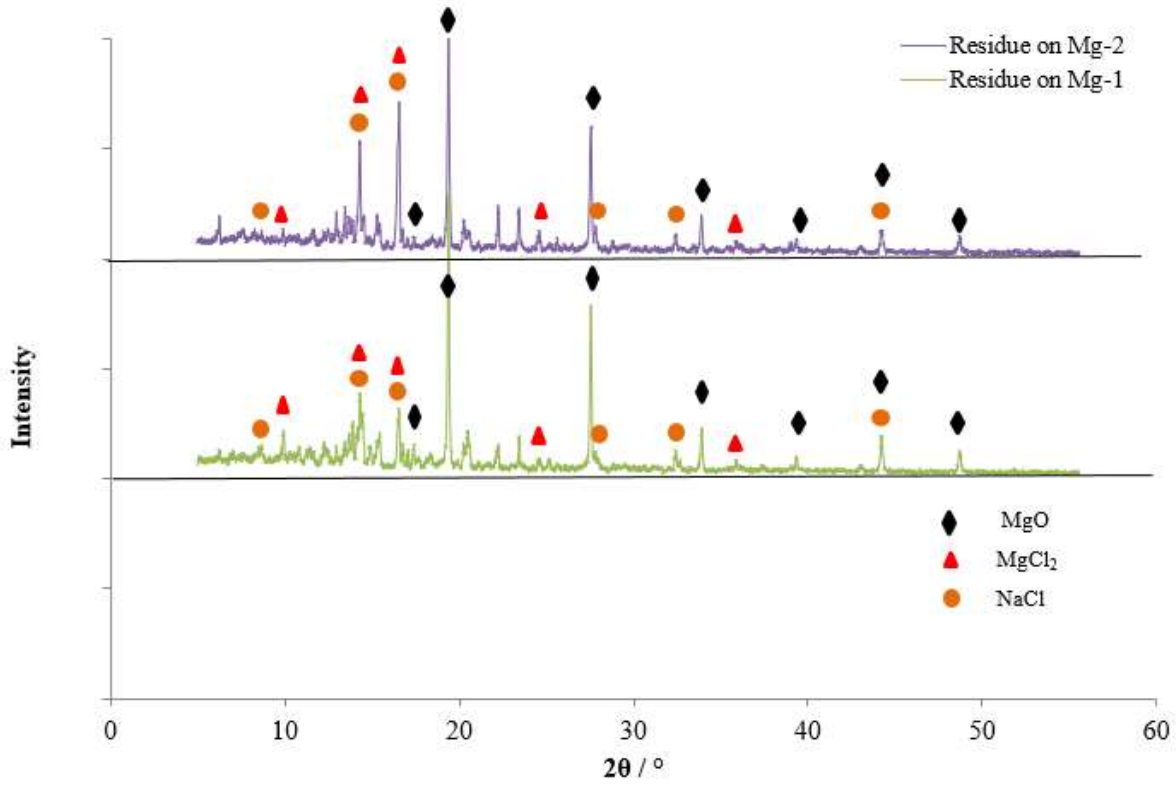

Figure 8: XRD of the residuals on Mg-1 and Mg-2 electrodes. Main components in the residuals are MgO and salts such as $MgCl_2$ and NaCl.

3.3. Effect of electrolytic salt purification on molten chloride salt

Before and after the salt purification, the concentration of the main corrosive impurity $MgOH^+$ was measured with CV, while the corrosion rate of the Incoloy 800 H electrode immersed in the molten salt was measured with PDP. In Figure 9, CV measurements on the molten salt before and after the salt purification show that the current of the peak representing the reduction reaction of $MgOH^+$ (I_p) was reduced from 50 to 25 mA (~50% reduction), i.e., the peak current density (current of the peak I_p / contact area of W work electrode with molten salt ~16.5 mm^2) decreased from 314 to 157 mA/cm^2. Since the bulk concentration of $MgOH^+$ is proportional to the peak current density with the slope of 97.9±19.5 ppm/(mA/cm^2) (38.2±7.6 ppm O/ mA/cm^2 as reported in our previous work [42]), the concentration of $MgOH^+$ in the molten salt was reduced from 30592±6123 ppm to 15296±3062 ppm (~50% reduction) according to CV measurements. Considering the total mass of the molten salt (~140 g), ~2.14±1.29 g $MgOH^+$ was reduced by the salt purification. From Figure 6, the total amount of electrical charge flowing in the 2 hours electrolysis was determined to be ~600 C by calculation with the following equation:

Total amount of electrical charge q (coulomb, C) = Current (A) × Time (s).

This represents ~6.2 mmol transferred electrons (Faraday constant 96485 C/mol) or 3.1 mmol (74.4 mg) reacted magnesium (reaction (II)). Assuming all the transferred electrons were related to the reduction reaction of $MgOH^+$ (i.e., Reaction (I) in Section 3.1), 6.2 mmol (0.25 g) $MgOH^+$, which is only ~12 % of the total amount of reduced $MgOH^+$ determined with CV measurements (~2.14±1.29 g).

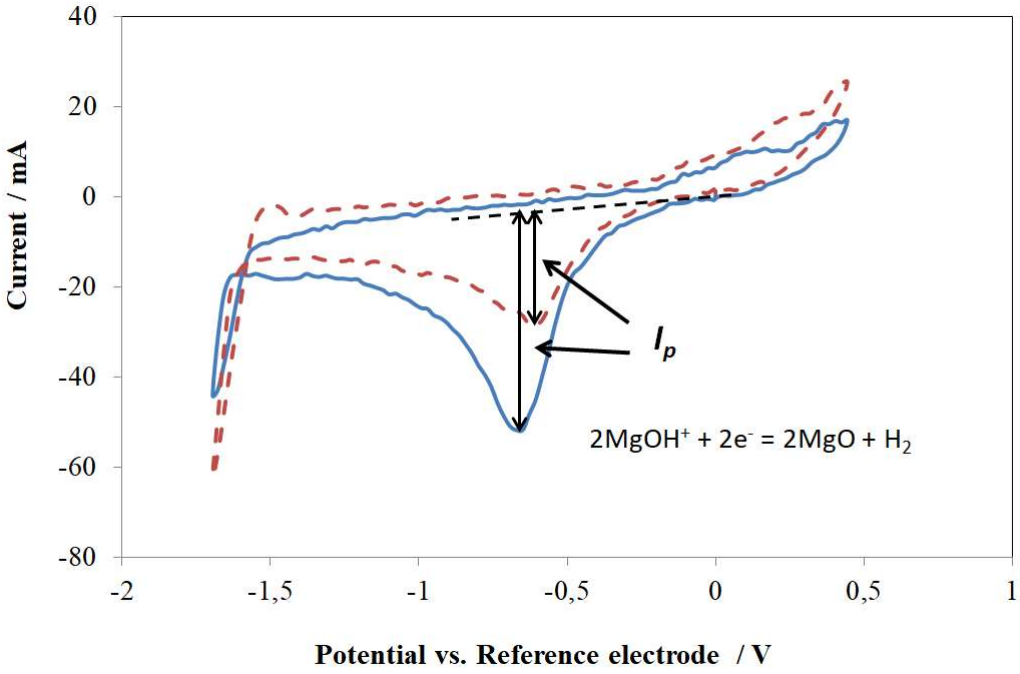

Figure 9: CV diagrams of molten salt at 500°C before (solid) and after (dashed) 2 h electrolysis experiment. Potential sweep rate: 200 mV/s; Working electrode: tungsten. W quasi-reference electrode was used.

The total mass loss of the both magnesium electrodes was weighed after the experiment to be about ~120 mg (~61 mg for Mg-1 and ~59 mg for Mg-2), more than the reacted magnesium calculated from the total amount of electrical charge flowing in the electrolysis (74.4 mg). This might be due to e.g., the spontaneous reaction of Mg with the impurity before and during the experiment, as described in one of our previous publications with Mg treatment without applied voltage [39]. Assuming all the reduced Mg of the both magnesium electrodes (~120 mg) for reaction with $MgOH^+$, 0.41 g $MgOH^+$ is calculated to react with Mg, which is ~19% of the total amount of reduced $MgOH^+$. Thus, besides the electrolysis and the spontaneous reaction of Mg with $MgOH^+$, the thermal decomposition of $MgOH^+Cl^-$ to MgO (precipitate) and HCl (gas) [8,35-36] could also contribute to the reduction of the $MgOH^+$ concentration. For a comparison, the reduced amounts of $MgOH^+$ due to the aforementioned factors are summarized in Table 3. Due to e.g., limited electrolysis rate (limited electrode surface or electrode passivation), more than 80% reduced $MgOH^+$ was caused by thermal decomposition or others, which may produce corrosive HCl gas.

Although the electrolytic salt purification method with two Mg-electrodes in this work shows great improvement in electrolysis duration (i.e., reduction of electrode passivation) compared to that reported in previous work with Mg- and W-electrodes [24], its electrolysis rate and duration should be further improved by optimizing the electrolysis conditions and the electrodes (their geometry with a large surface), or introduction of mechanical cleaning of the electrodes.

Table 3: Comparison of reduced amount of $MgOH^+$ due to electrolysis, spontaneous reaction and others (e.g., thermal decomposition).

Factor for reduction of $MgOH^+$ amount	**Reduced $MgOH^+$ / g**
Electrolysis (electrochemical)	~0.25 (~12%)
Spontaneous reaction with Mg (chemical)	~0.16 (~7%)
Thermal decomposition (thermal) or others	~1.73 (~81%)
Total (CV results)	**~2.14±1.29 (100%)**

As reported in literature [11, 24], the reduced concentration of the impurities like $MgOH^+$ can lead to reduced corrosivity of the molten salt. Figure 10 shows the PDP curves of In 800H immersed in the molten salt at 500°C before and after the electrolysis. Before the salt purification, the PDP curve shows that the corrosion current determined with the Tafel slopes is ~10 mA. With this corrosion current, the corrosion rate is estimated to be ~14.97 mm/year according to the method reported in [24]. In the purified salt after the electrolysis, the corrosion current is reduced to ~2.82 mA, i.e., the corrosion rate is significantly reduced to be ~4.19 mm/year (~72% reduction). Moreover, the corrosion potential (i.e., redox potential of the molten salt) decreased from -85 to -93 mV. Note that, PDP is an estimation method for in-situ qualitative investigation of the corrosion behavior. Table 4 summarizes all the results of CV and PDP for comparison.

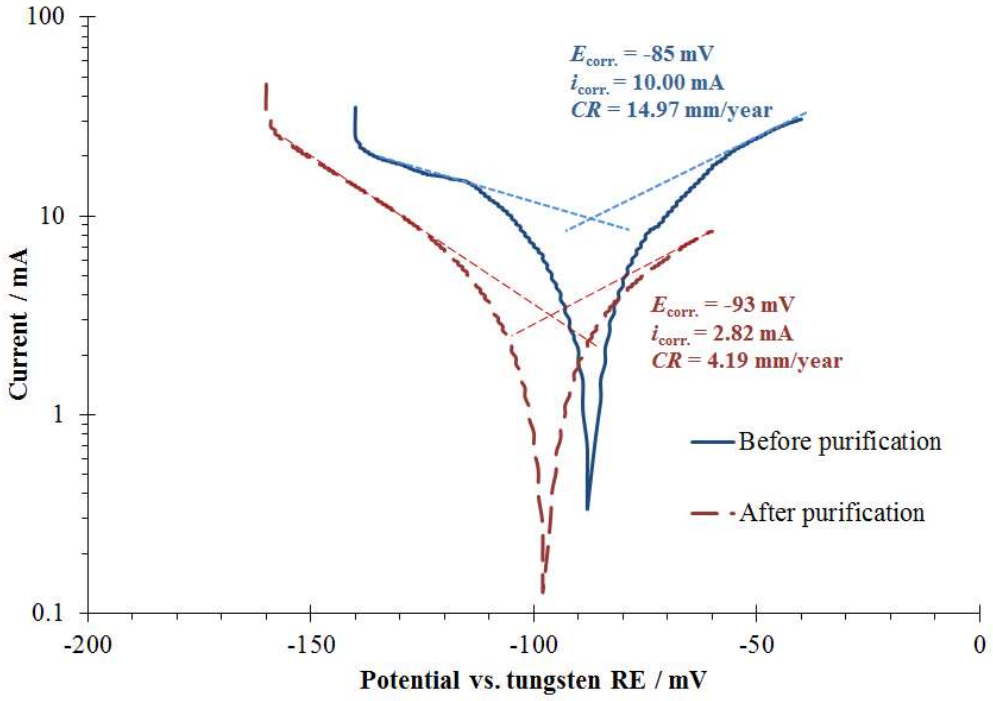

Figure 10: PDP curves of In 800 H immersed in the molten salt at 500°C before (solid) and after (dashed) electrolysis. W quasi-reference electrode was used.

Table 4: Corrosive current, corrosion potential and calculated corrosion rate of In 800 H in molten salt before and after salt purification.

	Tests	Non-purified salt	Purified salt
CV	Peak Current I_p (mA)	50	25
	Peak current density (mA/cm^2)	314	157
	C($MgOH^+$) (ppm)	30592±6123	15296±3062 (~50% reduction)
PDP (In 800 H)	Corrosion potential / mV	-85	-93
	Corrosion current / mA	10.00	2.82
	Corrosion rate / (mm/year)	14.97	4.19 (~72% reduction)

3.4. Comparison and recommendations of salt purification methods for molten chlorides

As mentioned in the section of Introduction and shown in Table 3, the corrosive impurities in the molten chloride salts can be reduced by chemical, thermal or electrochemical salt purification methods. In this section, the advantages and disadvantages of the salt purification methods available in literature, as well as the recommendation of their applications in the molten chloride TES system are discussed and summarized in Table 5.

With the chemical salt purification by e.g., bubbling the reducing gases like CCl_4 [11] or adding the reducing solids/liquids like Mg [31,39], the concentration of the corrosive impurity can be reduced to a very low level (<5 ppm O [11]). In such chemically purified salts, the commercial alloys like SS alloys and Ni-based alloys have a very low corrosion rate (<30 μm/year) in the molten chloride salt at 700°C [11]. Compared to other methods, the chemical methods have shown good purification effect on the salt with a wide range of impurity concentrations [11,31,39]. However, chemical methods have the disadvantage of requiring for large amounts of costly high purity, or sometimes harmful and toxic chemicals. Thus, they are suggested to be applied in e.g., pre-melting of the salt, accident in operation like air leakage, and corrosion control of the salt (control of molten salt chemistry) in operation.

In the thermal salt purification by e.g., stepwise heating of the hydrated salt [35-36, 46], only the thermal energy (i.e., heat) is needed. Several studies and this work have shown that it is effective and low-cost in releasing most of the hydrated water and hydrolysis products (e.g., MgOHCl) in the chloride salt when the impurity concentration is high [35-36, 46]. Thus, they are generally more economic than other methods for salt pre-purification. However, they are not effective for reducing impurity levels to the ppm-range due to mass transfer and thermodynamic limitations [35, 46]. Moreover, the small amount of residual water after thermal treatment (e.g., the last hydrated water in $MgCl_2 \cdot H_2O$) cannot be removed without decomposition, since the hydrolysis reaction takes place [18]. Because of this, a large amount of toxic and/or corrosive gases like HCl is produced by the dehydration reactions and has to be treated before being released to the environment. Therefore, the application in pre-melting of the salt is suggested to economically remove most of the hydrated water.

In the electrochemical salt purification by electrolysis with inert (e.g. W) or active (e.g. Mg, C) electrodes [24, 41, 45], the use of energy (electricity) and materials (electrodes) can have a higher efficiency due to enhanced reaction kinetics and controllable reaction equilibriums by controlling the voltage, compared to the aforementioned thermal and chemical methods. For instance, this method can reduce the concentrations of the impurities to very low levels by applying a high voltage. Moreover, the production of toxic gases like HCl and Cl_2 can be avoided by using active electrodes, e.g., in this work, only H_2 is produced. Thus, it is suggested to be used in the final salt purification after pre-purification and corrosion control of the molten salt in operation. Compared to other methods, this method is more complex due to the complex reaction system and process. More research effort is needed for realizing its application in the commercial molten chloride TES system.

Table 5: Comparison of salt purification methods for molten chlorides available in literature.

Methods	Advantage	Disadvantage	Recommended applications
Chemical	• Effective for a wide range of impurity concentration • Sufficient low impurity levels can be achieved	• Not cheap, toxic or not environmentally friendly chemicals needed	• Pre-melting of the salt • Corrosion control of the salt in operation • Accident in operation like air leakage
Thermal	• Simplicity and economic (Only heat needed) • Effective for dehydration	• Not effective for impurity removal at low concentration due to diffusion and thermodynamic limitations • Toxic gases like HCl produced • For $MgCl_2$ not all crystal water can be removed without HCl release	• Pre-melting of the salt (large amount)
Electrochemical	• High efficiency of use of energy and materials • Enhanced reaction kinetics and controllable reaction equilibriums • Effective for low impurity concentration • Toxic gases like HCl and Cl_2 avoided	• May be not effective for high impurity concentration due to fast electrode passivation • Complexity of purification process	• Final salt purification after pre-purification • Corrosion control of the salt in operation

4. Conclusions

An electrolytic salt purification method using two Mg electrodes and alternating voltage (AV) has been investigated to purify the molten $MgCl_2$-KCl-NaCl chloride salts. The concentration

of the corrosive impurity $MgOH^+$, and thus corrosivity of the molten chloride salts, was reduced effectively. Compared to other methods available in literature, the use of energy (electricity) and materials (electrodes) can have a higher efficiency due to enhanced reaction kinetics and controllable reaction equilibriums by controlling the voltage and using the active Mg electrodes. To our best knowledge the electrolytic salt purification in this work was investigated for the first time. Based on this improved electrolytic salt purification method, a German patent [47] has been filed.

The main conclusions of this work are:

- Compared to the salt purification method reported in our previous work [24], this method shows great improvement regarding the electrode duration due to electrode passivation with MgO.
- The MgO-spalling mechanism of this improved salt purification method is proposed and investigated experimentally.
- By reducing the corrosive impurity with the electrolytic salt purification, indicative PDP measurements show that the corrosion rate of Incoloy 800 H in the molten salt at 500°C can be reduced by ~72%.
- The advantages and disadvantages of the chemical, thermal and electrochemical salt purification methods, as well as the recommendation of their applications in the molten chloride TES system are given.

Some future work is suggested:

- The electrolysis should be investigated with different time intervals and voltages for optimization.
- The electrolysis could produce the nano-MgO particles in the molten salts, i.e., nano-fluids. Besides the viscosity, other thermal properties of the molten salt such as specific heat capacity and thermal conductivity could be changed significantly [48]. The effect of the existing nano-MgO particles will be studied.
- The reusable of the Mg rod or the life time of Mg rod electrodes as well as the ability of electrolysis will be studied by increasing the mass of salt and modifying the Mg electrodes, e.g., with a large surface.

Acknowledgments

This research has been performed within the DLR-DAAD fellowship programme (grant number 57265854), which is funded by German Academic Exchange Service (DAAD) and German Aerospace Center (DLR). The authors would like to thank their colleagues Dr. Carolina Villada

and Mr. Markus Braun at the DLR-Institute of Engineering Thermodynamics, Prof. Dr. Rainer Niewa, Mr. Sebastian Kunkel at the Institut für Anorganische Chemie, Universität Stuttgart, for their support.

References

1. M. Mehos, C. Turchi, J. Vidal, M. Wagner, Z. Ma, C. Ho, W. Kolb, C. Andraka, A. Kruizenga, Concentrating solar power Gen3 demonstration roadmap. National Renewable Energy Laboratory (NREL) Technical Report: NREL/TP-5500-67464, 2017.
2. G. Mohan, M. Venkataraman, J. Gomez-Vidal, J. Coventry, Assessment of a novel ternary eutectic chloride salt for next generation high-temperature sensible heat storage, Energy Convers. Manag. 167 (2018) 156-164.
3. X. Xu, X. Wang, P. Li, Y. Li, Q. Hao, B. Xiao, H. Elsentriecy, D. Gervasio, Experimental test of properties of KCl–$MgCl_2$ eutectic molten salt for heat transfer and thermal storage fluid in concentrated solar power systems. J. Sol. Energy Eng. 140(5) (2018) 051011 (9 pages).
4. Y. Li, X. Xu, X. Wang, P. Li, Q. Hao, B. Xiao, Survey and evaluation of equations for thermophysical properties of binary/ternary eutectic salts from NaCl, KCl, $MgCl_2$, $CaCl_2$, $ZnCl_2$ for heat transfer and thermal storage fluids in CSP, Sol. Energy 152 (2017) 57–79.
5. K. Vignarooban, X. Xu, A. Arvay, K. Hsu, A.M. Kannan, Heat transfer fluids for concentrating solar power systems – A review, Appl. Energy 146 (2015) 383-396.
6. J. Gasia, L. Miró, L.F. Cabeza, Review on system and materials requirements for high temperature thermal energy storage. Part 1: General requirements, Renew Sust. Energ. Rev. 75 (2017) 1320-1338.
7. X. Li, N. Li, W. Liu, Z. Tang, J. Wang, Unrevealing the thermophysical properties and microstructural evolution of $MgCl_2$–NaCl–KCl eutectic: FPMD simulations and experimental measurements, Sol. Energy Mater. Sol. Cells 210 (2020) 110504.
8. T. Xu, X. Li, L. Guo, F. Wang, Z. Tang, Powerful predictability of FPMD simulations for the phase transition behavior of NaCl-$MgCl_2$ eutectic salt, Sol. Energy 209 (2020) 568-575.
9. W. Ding, A. Bonk, T. Bauer, Corrosion behavior of metallic alloys in molten chloride salts for thermal energy storage in concentrated solar power plants - A review, Front. Chem. Sci. Eng. 12(3) (2018) 564–576.
10. US. Department of Energy (US): Generation 3 Concentrating Solar Power Systems (Gen3 CSP), Website: https://www.energy.gov/eere/solar/generation-3-concentrating-solar-power-systems-gen3-csp.
11. J.M. Kurley, P.W. Halstenberg, A. McAlister, S. Raiman, S. Dai, R.T. Mayes, Enabling chloride salts for thermal energy storage: implications of salt purity. RSC Adv. 9 (2019) 25602-25608.

12. J.C. Vidal, N. Klammer, Molten chloride technology pathway to meet the U.S. DOE SunShot initiative with Gen3 CSP. AIP Conference Proceedings, 2126 (2019) 080006.
13. H. Sun, P. Zhang, J. Wang, Effects of alloying elements on the corrosion behavior of Ni-based alloys in molten NaCl-KCl-$MgCl_2$ salt at different temperatures. Corros. Sci. 143 (2018)187-199.
14. X. Li, W. Liu, Z. Tang, J. Wang, Insight into dynamic interaction of molten $MgCl_2$-NaCl-KCl with impurity water via FPMD simulations, J. Mol. Liq. 314 (2020) 113596.
15. A.G. Fernandez, J. Gomez-Vidal, E. Oro, A. Kruizenga, A. Solé, L.F. Cabeza, Mainstreaming commercial CSP systems: A technology review. Renew. Energy 140 (2019) 152-176.
16. W. Ding, H. Shi, Y. Xiu, A. Bonk, A. Weisenburger, A. Jianu, T. Bauer, Hot corrosion behavior of commercial alloys in thermal energy storage material of molten $MgCl_2$/KCl/NaCl under inert atmosphere, Sol. Energy Mater. Sol. Cells 184 (2018) 22-30.
17. W. Ding, A. Bonk, T. Bauer, Molten chloride salts for next generation CSP plants: Selection of promising chloride salts & study on corrosion of alloys in molten chloride salts, AIP Conference Proceedings 2126 (2019) 200014.
18. G.J. Kipouros, D.R. Sadoway, A thermochemical analysis of the production of anhydrous $MgCl_2$, J. Light Met. 1(2) (2001) 111–117.
19. A.M. Kruizenga, Corrosion Mechanisms in Chloride and Carbonate Salts. SANDIA Report SAND2012-7594, 2012.
20. K. Vignarooba, P. Pugazhendhi, C. Tucker, D. Gervasio, A.M. Kannan, Corrosion resistance of Hastelloys in molten metal-chloride heat-transfer fluids for concentrating solar power applications, Sol. Energy 103 (2014) 62-69.
21. K. Vignarooban, X. Xu, K. Wang, E.E. Molina, P. Li, D. Gervasio, A.M. Kannan, Vapor pressure and corrosivity of ternary metal-chloride molten-salt based heat transfer fluids for use in concentrating solar power systems, Appl. Energy 159 (2015) 206-213.
22. G.Y. Lai, High-Temperature Corrosion and Materials Applications, Chapter 15 in book: Molten Salt Corrosion, ASM International, 2007.
23. S. Guo, J. Zhang, W. Wu, W. Zhou, Corrosion in the molten fluoride and chloride salts and materials development for nuclear applications, Prog. Mater. Sci. 97 (2018) 448-487.
24. W. Ding, J. Gomez-Vidal, A. Bonk, T. Bauer, Molten chloride salts for next generation CSP plants: Electrolytical salt purification for reducing corrosive impurity level, Sol. Energy Mater. Sol. Cells 199 (2019) 8-15.
25. D.F. Williams, Assessment of candidate molten salt coolants for the NGNP/NHI heat-transfer loop. Oak Ridge National Laboratory, 2006.

26. B. Liu, X. Wei, W. Wang, J. Lu, J. Ding, Corrosion behavior of Ni-based alloys in molten NaCl-$CaCl_2$-$MgCl_2$ eutectic salt for concentrating solar power, Sol. Energy Mater. Sol. Cells 170 (2017) 77–86.
27. V.L. Cherginets, T.P. Rebrova, Studies of some acid-base equilibria in the molten eutectic mixture KCl-LiCl at 700°C, Electrochim. Acta 45(3) (1999) 469-476.
28. L. Guo, Q. Liu, H. Yin, T.J. Pan, Z. Tang, Excellent corrosion resistance of 316 stainless steel in purified NaCl-$MgCl_2$ eutectic salt at high temperature, Corr. Sci., 2020, 166: 108473.
29. D.L. Maricle, D.N. Hume, A new method for preparing hydroxide-free alkali chloride melts, J. Electrochem. Soc. 107(4) (1960) 354-356.
30. J. Ambrosek, Doctoral thesis: Molten Chloride Salts for Heat Transfer in Nuclear Systems, in Nuclear Engineering and Engineering Physics, University of Wisconsin-Madison, 2011.
31. B.L. Garcia-Diaz, L. Olson, M. Martinez-Rodriguez, R. Fuentes, H. Colon-Mercado, J. Gray, High temperature electrochemical engineering and clean energy systems, J. South Carol. Acad. Sci. 14(1) (2016) Article 4.
32. B. Mishra, D.L. Olson, Corrosion of refractory alloys in molten lithium and lithium chloride, Min. Proc. Ext. Met. Rev. 22(4-6 SCPEC. ISS) (2001) 369-388.
33. J.E. Indacochea, J.L. Smith, K.R. Litko, E.J. Karell, A.G. Rarez, High-temperature oxidation and corrosion of structural materials in molten chlorides, Oxid. Met. 55(1-2) (2001) 1-16.
34. J.E. Indacochea, J.L. Smith, K.R. Litko, E.J. Karell, Corrosion performance of ferrous and refractory metals in molten salts under reducing conditions, J. Mater. Res. 14(5) (1999) 1990-1995.
35. L. Maksoud, T. Bauer, Experimental investigation of chloride molten salts for thermal energy storage applications. In: Proceedings of 10th International Conference on Molten Salt Chemistry and Technology, Shenyang, China, 2015, 273-280.
36. G.J. Kipouros, D.R. Sadoway, A thermochemical analysis of the production of anhydrous $MgCl_2$. J. Light Met. 1(2) (2001) 111–117.
37. J. Vidal. Corrosion resistance of MCrAlX coatings in a molten chloride for thermal storage in concentrating solar power applications. npj Mater. Degrad. 7 (2017) 1-9.
38. J.K. Bunn, R.L. Fang, M.R. Albing, A. Mehta, M.J. Kramer, M.F. Besser, J.R. Hattrick-Simpers, A high-throughput investigation of Fe–Cr–Al as a novel high temperature coating for nuclear cladding materials, Nanotechnology 26(27) (2015) 274003.
39. W. Ding, H. Shi, A. Jianu, Y. Xiu, A. Bonk, A. Weisenburger, T. Bauer, Molten chloride salts for high-temperature thermal energy storage: Mitigation strategies against corrosion of structural materials, Sol. Energy Mater. Sol. Cells 193 (2019) 298-313.
40. B. Jönsson, Q. Lu, D. Chandrasekaran, R. Berglund, F. Rave, Oxidation and creep limited lifetime of Kanthal APMT®, a dispersion strengthened FeCrAlMo alloy designed for strength and oxidation resistance at high temperatures, Oxid. Met. 79(1–2) (2013) 29–39.

41. W. Ding, A. Bonk, J. Gussone, T. Bauer, Cyclic voltammetry for monitoring corrosive impurities in molten chlorides for thermal energy storage, Energy Procedia 135 (2017) 82-91.
42. W. Ding, A. Bonk, J. Gussone, T. Bauer, Electrochemical measurement of corrosive impurities in molten chlorides for thermal energy storage, J. Energ. Storage 15 (2018) 408–414.
43. R.A. Skar, Doctoral Thesis: Chemical and Electrochemical Characterisation of Oxide/hydroxide Impurities in the Electrolyte for Magnesium Production, Norwegian University of Science and Technology (NTNU), 2001.
44. J. Gussone, Doctoral thesis: "Schmelzflusselektroytische Abscheidung von Titan auf Verstärkungsfasern zur Herstellung von Titanmatrixverbundwerkstoffen", RWTH Aachen University, Shaker Verlag Aachen, 2012.
45. Chinese Patent CN106283112A, The electrochemical purification method of fused salt, published on January 4th of 2017. Authors: W. Huang, F. Jiang, L. Tian, C. She, H. Zheng, D. long and Q. Li.
46. Y. Zhao, N. Klammer, J. Vidal, Purification strategy and effect of impurities on corrosivity of dehydrated carnallite for thermal solar applications, RSC Adv., 2019, 9, 41664-41671.
47. German Patent Application DE1020191073936 "Verfahrenstechnik für Halogensalze mit zwei identischen Elektroden" filed on March 22nd of 2019. Authors: W. Ding, F. Yang and T. Bauer (DLR).
48. X. Wei, X. Zhang, J. Ding, W. Wang, J. Lu, The effect of nano-MgO on thermal properties of ternary chloride fluid, Energy Procedia 158 (2019) 773-778.